

Supporting information for

Formamide-derived “glue” for hundred-gram scale synthesis of atomically dispersed iron-nitrogen-carbon electrocatalysts

Zongge Li^{a,b,†}, Yan Ma^{b,†}, Yiyan Wang^b, Nianxi Liu^a, Ying Zhang^{b,*}, and Guoxin Zhang^{a,*}

a. Al-ion Battery Research Center, Department of Electrical Engineering and Automation, Shandong University of Science and Technology, Qingdao, Shandong 266590, P. R. China. E-mail: zhanggx@sdust.edu.cn.

b. State Key Laboratory of Heavy Oil Processing, China University of Petroleum (East China), Qingdao, Shandong 266580, P. R. China. E-mail: yzhang@upc.edu.cn.

† These authors contribute equally to this work.

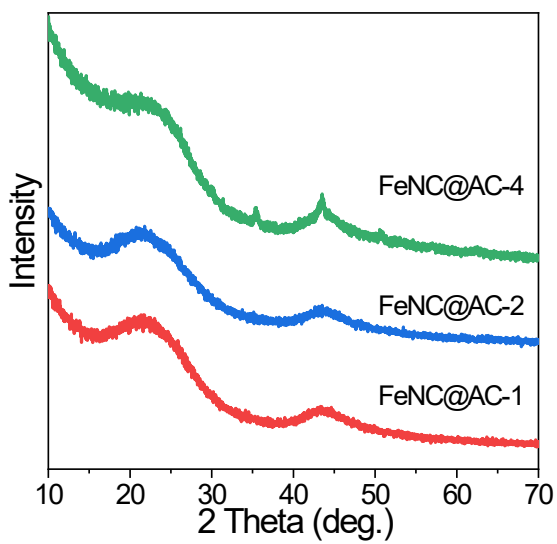


Figure S1. XRD curves of FeNC@AC-X, X=1, 2, or 4.

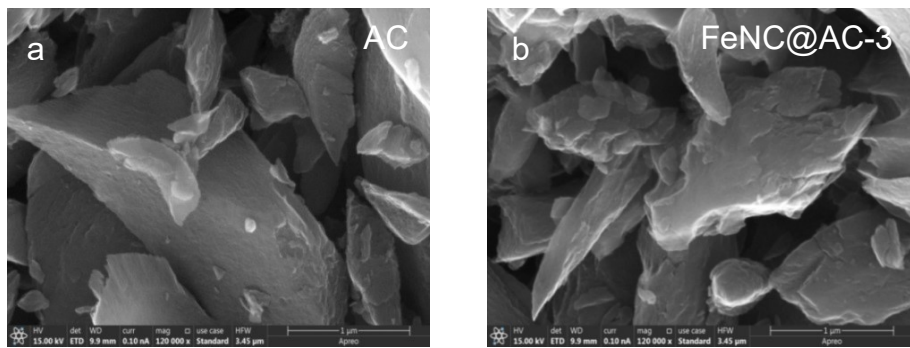


Figure S2. SEM images of (a) activated carbon black (AC) and (b) FeNC@AC samples.

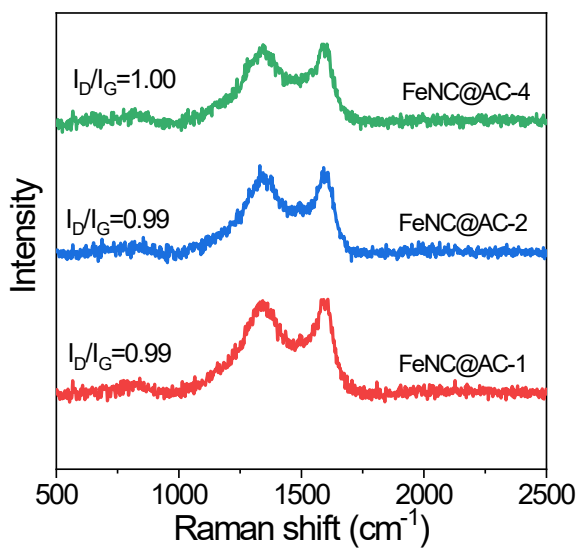


Figure S3. Raman spectra of FeNC@AC-X, X=1, 2, or 4.

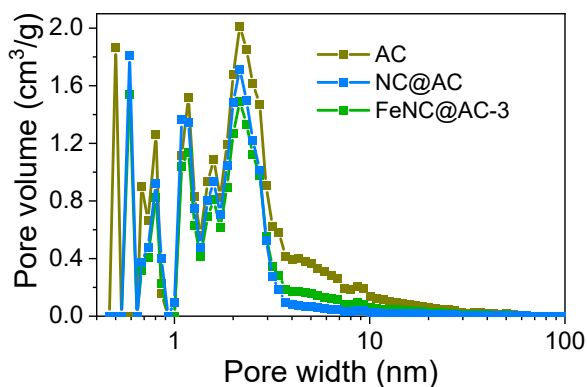


Figure S4. Pore distribution curves of AC, NC@AC, and FeNC@AC-3.

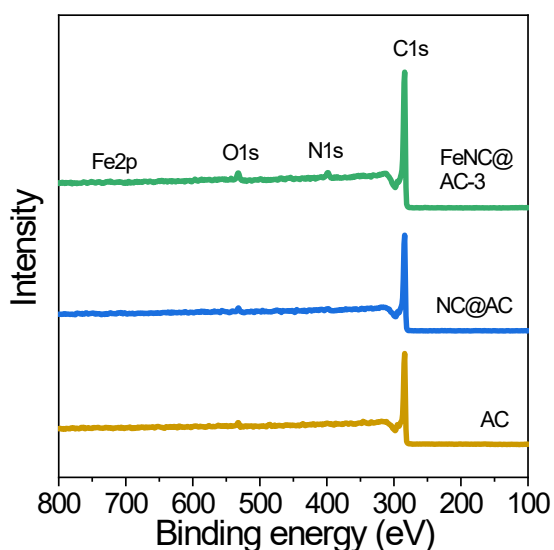


Figure S5. XPS survey curves of AC, NC@AC, and FeNC@AC-3.

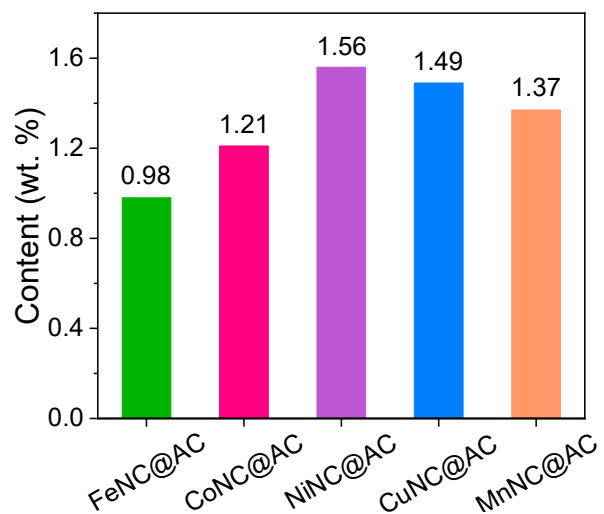


Figure S6. ICP element weight percentages of FeNC@AC, and other four types of as-made MNC@AC materials.

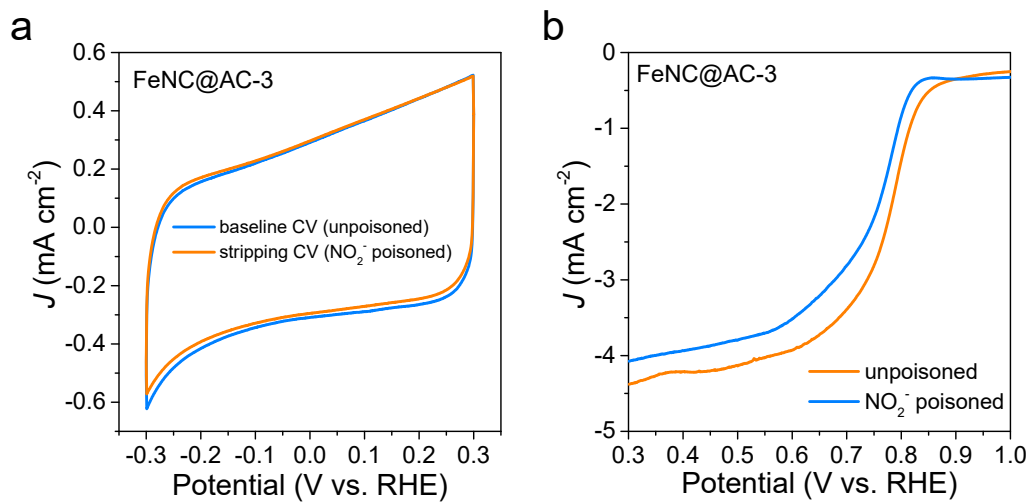


Figure S7. Determination of site density of FeNC@AC-3 through reversible nitrite poisoning. (a) CV curves and (b) ORR LSV curves before and after nitrite adsorption in a 0.5 M acetate buffer at pH 5.2.

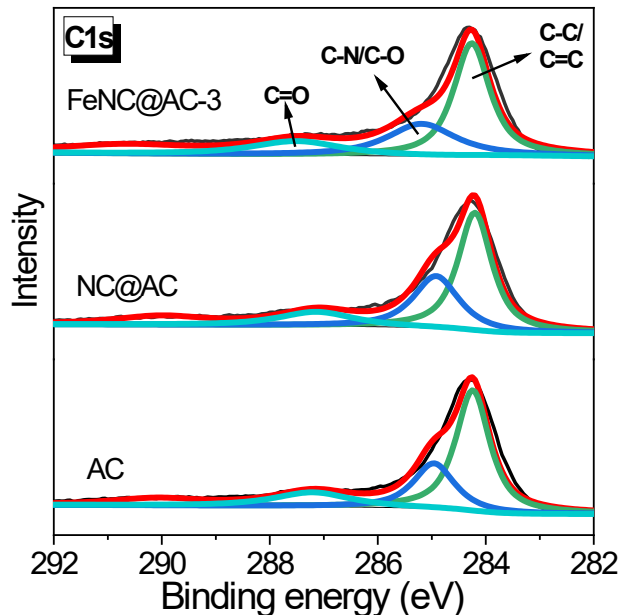


Figure S8. (a) XPS survey curves and (b) C1s spectra of AC, NC@AC, and FeNC@AC-3.

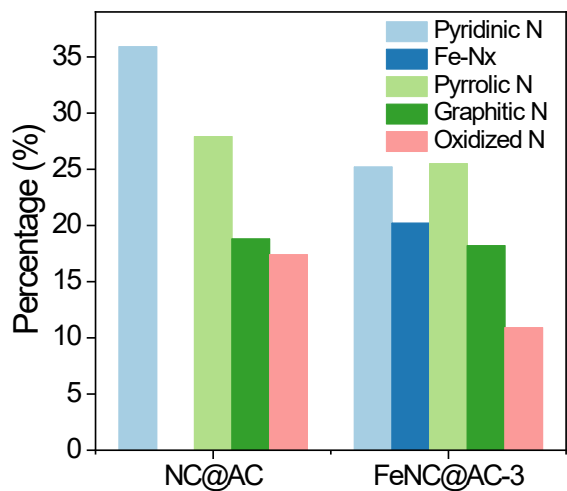


Figure S9. Percentages of different N species in NC@AC and FeNC@AC-3.

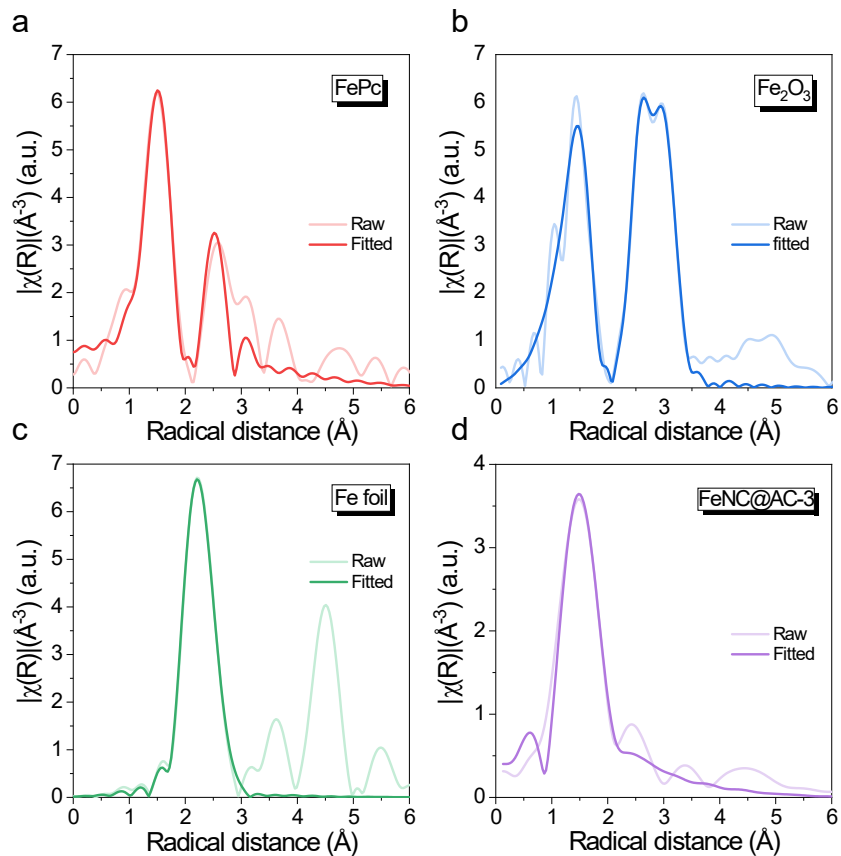


Figure S10. Fe K-edge EXAFS fitting curves of (a) FePc, (b) Fe_2O_3 , (c) Fe foil, and (d) FeNC@AC-3 in R-space.

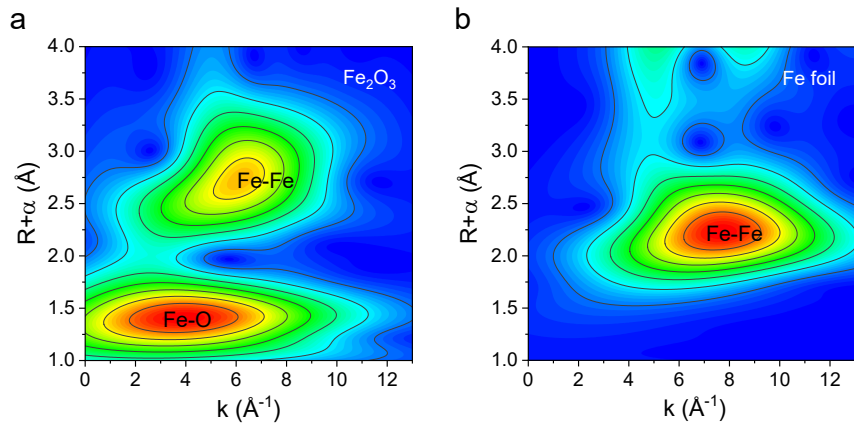


Figure S11. Wavelet transformed (WT) EXAFS spectra of (a) Fe_2O_3 and (b) Fe foil.

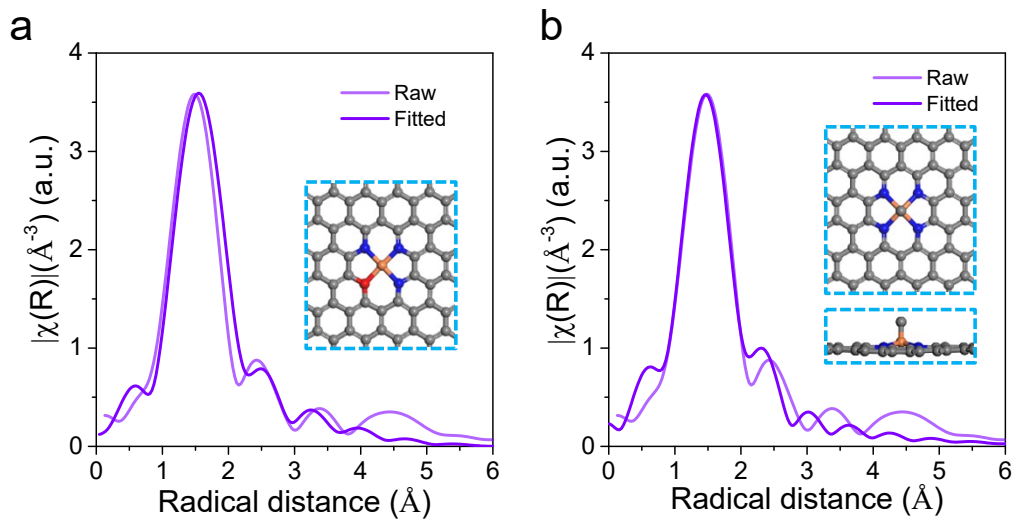


Figure S12. Fe k-edge EXAFS fitting curves of (a) $\text{Fe}-\text{N}_3\text{O}_1$ and (b) $\text{C}-\text{Fe}-\text{N}_4$ in R-space, insets show their corresponding proposed coordination structures.

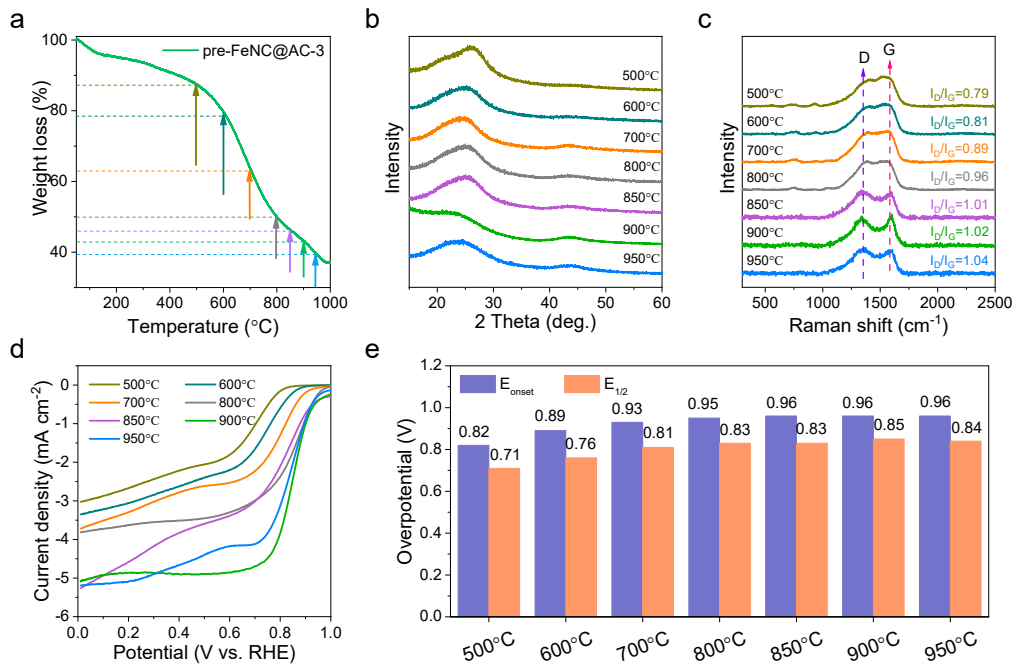


Figure S13. (a) TGA curve of pre-FeNC@AC-3. (b) XRD curves and (c) Raman spectra of Fe-NC@AC-3 synthesized at different temperatures. (d) ORR polarization curves of FeNC@AC-3 synthesized at different temperatures. Panel (e) shows a summary of onset potentials and half-wave potentials of Fe-NC@AC-3 synthesized at different temperatures.

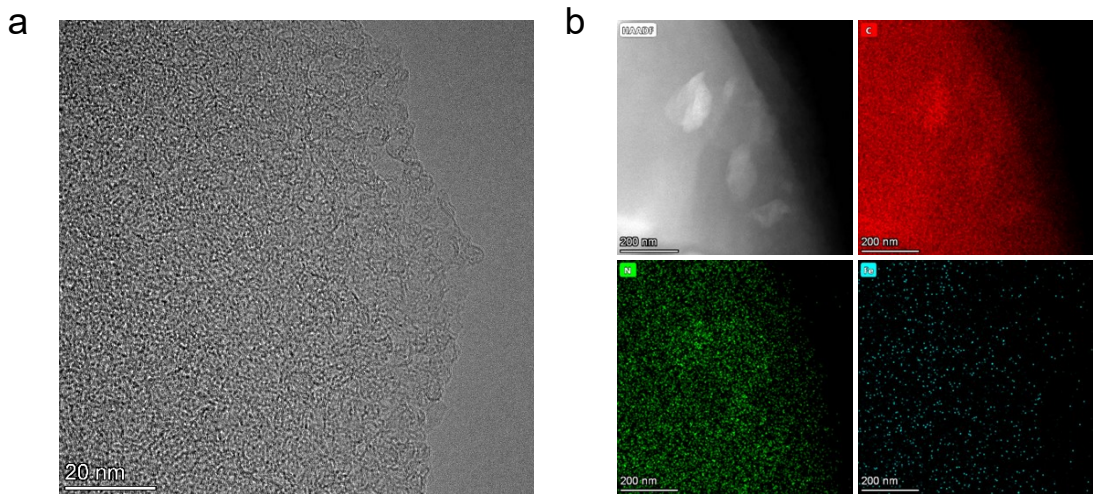


Figure S14. HRTEM image and EDS mapping images of FeNC@AC-3 after durability test.

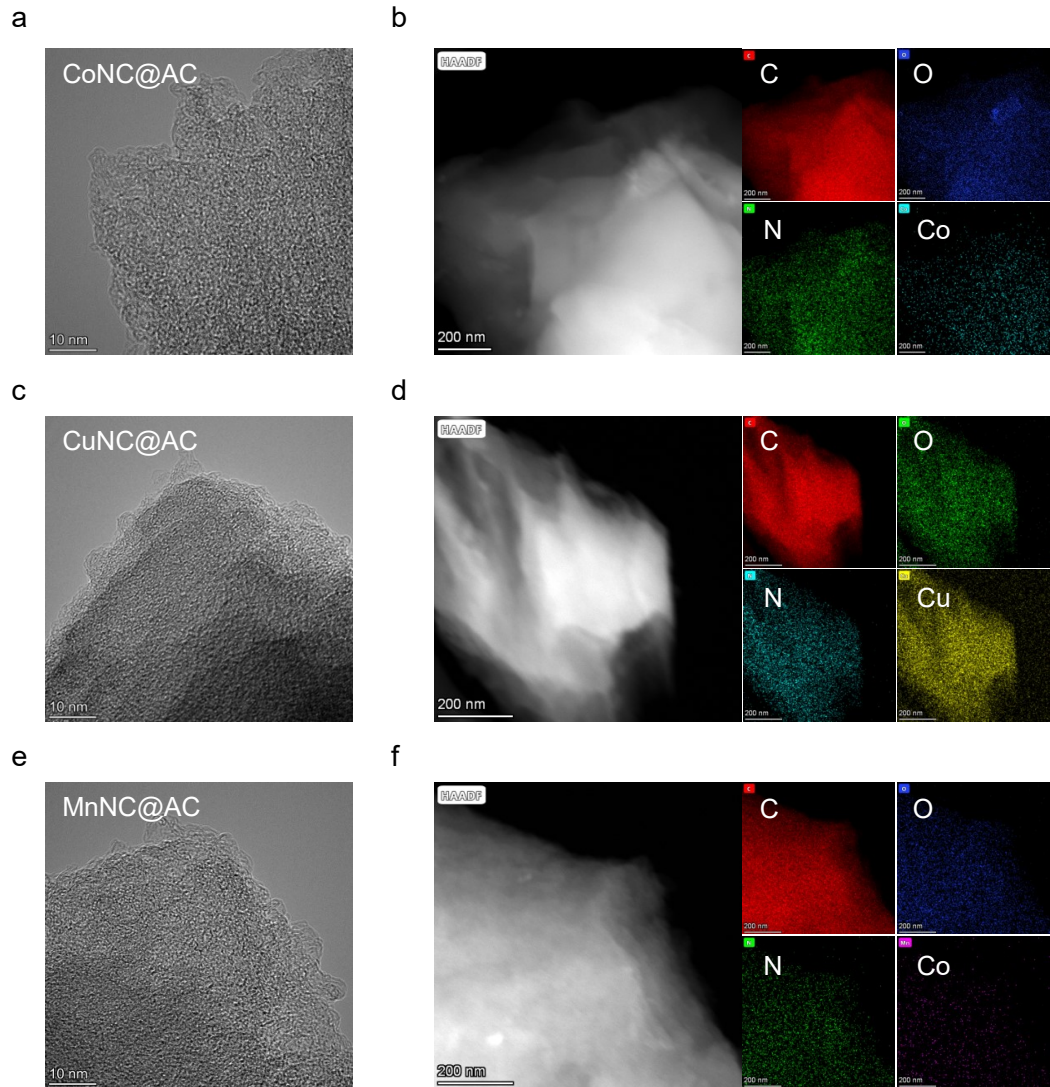


Figure S15. (a) HRTEM and (b) elemental mapping images of CoNC@AC sample. (c) HRTEM and (d) elemental mapping images of CuNC@AC sample. (e) HRTEM and (f) elemental mapping images of MnNC@AC sample.

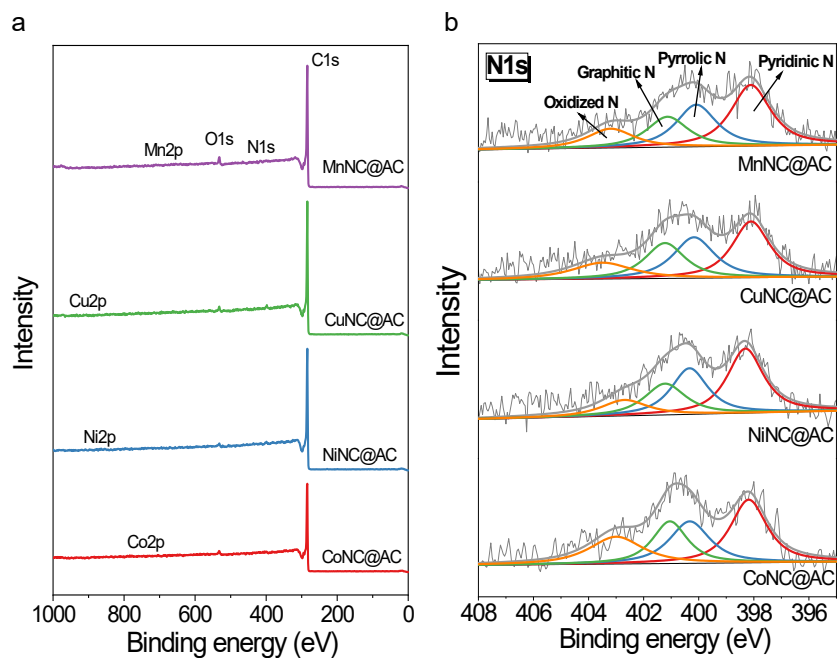


Figure S16. (a) XPS survey curves and (b) C1s spectra of CoNC@AC, NiNC@AC, CuNC@AC, and MnNC@AC.

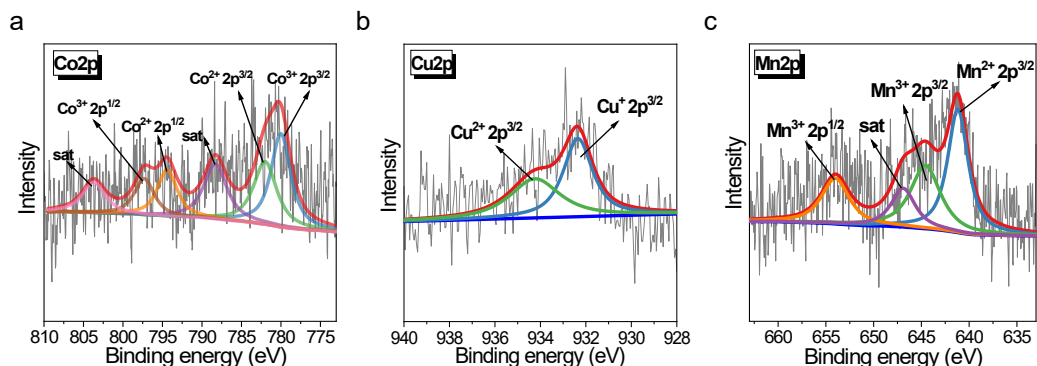


Figure S17. (a) Co2p spectra of CoNC@AC, (b) Cu2p spectra of CoNC@AC, and (c) Mn2p spectra of MnNC@AC

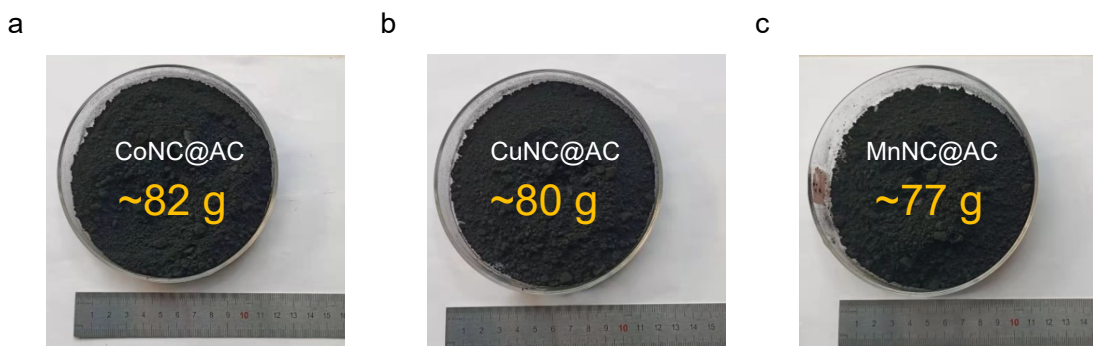


Figure S18. Digital image of appearance of (a) CoNC@AC, (b) CuNC@AC, and (c) MnNC@AC.

Table S1. XPS elemental analysis of AC, NC@AC, and FeNC@AC-3.

Sample	%C	%N	%O	%Fe
AC	97.33	0.39	2.28	-
NC@AC	95.25	2.1	2.65	-
FeNC@AC-3	93.99	1.45	4.38	0.19

Table S2. A summary of site density (SD), turnover of frequency (TOF), and Fe utilization rate of FeNC@AC-3 before and after long-term use (10,000 s).

Sample	Site density (SD)/site g ⁻¹	Turnover of frequency (TOF)/s ⁻¹	Utilization rate (%)
FeNC@AC-3	1.49×10 ¹⁹	1.69	16.0% (based on XPS) 14.9% (based on ICP)
FeNC@AC-3 after long- term use (10,000 s)	1.36×10 ¹⁹	1.57	14.6% (based on XPS) 12.9% (based on ICP)

Table S3. EXAFS fitting parameters at the Fe K-edge for the FeNC@AC-3 sample with comparison to standard references of Fe foil, Fe_2O_3 , and FePc. Comparison of $\text{Fe}-\text{N}_3\text{O}_1$ and $\text{C}-\text{Fe}-\text{N}_4$ to $\text{Fe}-\text{N}_4$ coordination are also shown.

Sample	Shell	N ^a	R(Å) ^b	$\sigma^2 \times 10^3 (\text{\AA}^2)$ ^c	ΔE_0 (eV) ^d	R factor
Fe foil	Fe-Fe	8*	2.47±0.01	4.8±0.8	6.7±1.3	0.001
	Fe-Fe	6*	2.85±0.01	6.0±1.7	5.4±2.6	
Fe_2O_3	Fe-O	6.1±1.1	1.93±0.02	11.7±2.7	-6.5±3.0	0.014
	Fe-Fe	2.6±1.4	2.99±0.05	9.8±4.9	-4.1±6.2	
FePc	Fe-Fe	8.4±4.1	3.42±0.02	10.3±3.3	-7.9±3.3	0.012
	Fe-N	4.1±0.5	1.99±0.02	8.0±3.0	8.1±3.2	
Fe in $\text{Fe}-\text{N}_4$ for FeNC@AC-3	Fe-C	4.8±2.1	2.98±0.02	6.7±3.4	7.4±3.3	0.016
	Fe-N	3.8±0.5	1.98±0.02	5.7±4.4	-3.8±2.9	
Fe in FeN_3O structure	Fe-N	3.1±0.3	1.97±0.05	6.8±4.6	-3.7±0.8	0.214
	Fe-O	1.2±0.3	2.03±0.09			
Fe in $\text{C}-\text{FeN}_4$ structure	Fe-C	4.9±0.6	1.99±0.06	3.3±2.7	-4.5±1.2	0.158

^aCN: coordination numbers; ^bR: bond distance; ^c σ^2 : Debye-Waller factors; ^d ΔE_0 : the inner potential correction. R factor: goodness of fit. S_0^{-2} was set to 0.729 (Fe), according to the experimental EXAFS fit of metal foil reference by fixing CN as the known crystallographic value.

Table S4. XPS elemental analysis of CoNC@AC, NiNC@AC, CuNC@AC, and MnNC@AC.

Sample	%C	%N	%O	%M (M=Co, Ni, Cu, and Mn)
CoNC@AC	96.72	1.16	1.90	0.22
NiNC@AC	95.95	1.34	2.5	0.21
CuNC@AC	95.8	1.54	2.49	0.16
MnNC@AC	94.56	1.12	4.1	0.22